



Swansea University  
Prifysgol Abertawe



## Cronfa - Swansea University Open Access Repository

---

This is an author produced version of a paper published in :

Cronfa URL for this paper:

<http://cronfa.swan.ac.uk/Record/cronfa8275>

---

### Conference contribution :

Essa, E., Xie, X., Sazonov, I., Nithiarasu, P. & Smith, D. (2011). *Automatic Segmentation of IVUS Media-Adventitia Border with Shape Prior.*

[http://dx.doi.org/ na](http://dx.doi.org/na)

---

This article is brought to you by Swansea University. Any person downloading material is agreeing to abide by the terms of the repository licence. Authors are personally responsible for adhering to publisher restrictions or conditions. When uploading content they are required to comply with their publisher agreement and the SHERPA RoMEO database to judge whether or not it is copyright safe to add this version of the paper to this repository.

<http://www.swansea.ac.uk/iss/researchsupport/cronfa-support/>

# Automatic Segmentation of IVUS Media-Adventitia Border with Shape Prior

Ehab Essa<sup>1</sup>  
csehab@swansea.ac.uk

Xianghua Xie<sup>1</sup>  
X.Xie@swansea.ac.uk

Igor Sazonov<sup>2</sup>  
I.Sazonov@swansea.ac.uk

Perumal Nithiarasu<sup>2</sup>  
P.Nithiarasu@swansea.ac.uk

Dave Smith<sup>3</sup>  
Dave.Smith@abm-tr.wales.nhs.uk

<sup>1</sup> Department of Computer Science  
Swansea University, UK

<sup>2</sup> College of Engineering  
Swansea University, UK

<sup>3</sup> ABM University NHS Trust  
Swansea, UK

---

## Abstract

We present a fully automatic segmentation method to extract media-adventitia border in IVUS images with shape prior information. Segmentation of IVUS has shown to be an intricate process due to relatively low contrast and various forms of interferences and artefacts caused by, for instance, calcification and acoustic shadow. We incorporate shape prior with an automatic graph cut technique to prevent the extraction of media-adventitia border from being distracted by those image features. Novel cost functions are constructed based on a combination of complementary texture features. Comparative studies on manually labeled data show promising performance of the proposed method.

## 1 Introduction

Intra-vascular ultrasound (IVUS) is a catheter based technology that provides 2D cross-sectional coronary vessel images to help clinicians to diagnose coronary heart diseases, such as atherosclerosis. There are two types of borders of clinical interest: the lumen-intima border that corresponds to the inner coronary arterial wall and the media-adventitia border that represents the outer coronary arterial wall located between the media and adventitia. Segmentation of the second type of border is the focus of this paper. The media layer is largely consisted of homogeneous smooth muscle, which exhibits as a dark layer in ultrasound images, and is surrounded by fibrous connective tissues called adventitia.

The appearance of the media-adventitia border in IVUS images is affected by various forms of imaging artefacts, such as acoustic shadow caused by catheter guide wire or tissue calcification. The use of shape prior is often desirable in order to achieve robust segmentation of those anatomical structures from IVUS images. For example, in [2] signed distance transform is used to implicitly represent prior shapes, followed by principal component analysis (PCA) to generalise the shape variation. The learned mean shapes (principal components) and their corresponding variations are then used to constrain image gradient based media-adventitia border segmentation. However, this method need specific tuning and shape training to work properly on high frequency ultrasound images, e.g. 40 MHz in

our case. Its global shape prior learning requires a general assumption that the shape variation is largely linear. Additionally, this kind of image gradient based approach may suffer from distraction of strong image features due to fibrous plaque and other imaging artefacts.

In this paper, we propose a fully automatic media-adventitia border segmentation method using graph cut and local shape prior. Multi-scale textural features are used to construct the cost function for graph partition. The use of local shape prior may allow a more flexible global shape variation. Evaluation of the proposed method is carried out on a manually labelled IVUS dataset. Substantial improvements are shown compared to segmentation without using the local shape prior.

## 2 Proposed method

The proposed method begins with some pre-processing which involves transforming the IVUS images from Cartesian coordinates to polar coordinates for the purpose of graph construction and automatic removal of catheter region from the transformed images since that region does not contain any anatomical information. All the training shapes which in polar coordinates are aligned by using rigid translation. The first order derivatives in radial distance are used to characterise the shape variation. Note, it is not generalising shape variation at each column, which requires for instance the training shapes to be generally in the same scale. Rather the variation in neighbouring inter-column changes are modelled and used in graph construction and partition. A node-weighted directed graph is constructed, taking into account the shape constraint. The segmentation of the media-adventitia border is thus considered as searching for a minimum closed set on this node-directed graph, which is solved by computing a minimum  $s-t$  cut in a derived arc-weighted directed graph. The associated cost function is based on image features extracted using local phase transform, first order derivatives of Gaussian, and Gabor filters. Finally, the extracted media-adventitia border is smoothed using efficient 1D radial basis function (RBF) interpolation.

### 2.1 Graph Construction

Conventional graph cut, such as [1], generally minimises an edge based energy function to find the optimal segmentation of IVUS, but it may fail due to the absence of strong coherent features along the border and the presence of distractive objects with similar intensity profiles. In [5], the authors incorporated some shape prior to overcome these problems. However, user initialisation is necessary. In [3], a novel graph construction method is proposed, which transforms surface segmentation in 3D into computing a minimum closed set in a directed graph. Very recently in an extended work [4], the arcs between neighbouring columns are set to be dynamic in order to incorporate prior shape and new arcs are added to constrain the smoothness of the interface. Here, we adopt this graph construction technique to carry out IVUS 2D segmentation, which achieves global minima in low order polynomial time complexity but does not require user initialisation.

Briefly, a graph  $G = \langle V, E \rangle$ , where each node  $V(x, y)$  corresponds to a pixel in image  $I(x, y)$ , is constructed for segmenting the media-adventitia interface  $S(x, y)$ . Along each column in the graph, every node is connected to the node below in the same column with  $+\infty$  weight on the arc to ensure that the desired interface intersects with each column exactly once. In the case of the inter-column arcs, for each node  $V(x, y)$  a directed arc with  $+\infty$  weight is established to link with node  $V(x+1, y - \bar{\Delta}_{p,q})$ , where  $\bar{\Delta}_{p,q}$  is the maximum difference between two neighbouring columns  $p$  and  $q$ . Similarly, node  $V(x+1, y)$  is connected to  $V(x, y + \underline{\Delta}_{p,q})$ , where  $\underline{\Delta}_{p,q}$  controls the minimum difference between two neighbouring columns. Without using the shape prior, the value for  $\bar{\Delta}_{p,q}$  and  $\underline{\Delta}_{p,q}$  are set as global constants for every pair of neighbouring columns and act as a hard constraint to prevent drastic

changes in shape. The neighbouring nodes in the last row are connected to each other with  $+\infty$  weight on arc to maintain a closed graph.

## 2.2 Shape Prior

Taking into account the shape constraint, the associated energy function used to find the optimal interface  $S$  can be defined as:

$$E(S) = \sum_{I(x,y) \in S} C(x,y) + \sum_{(p,q)} f_{p,q}(S(p) - S(q)) \quad (1)$$

where  $C(x,y)$  is the cost function, described in Sect. 2.4, and  $f_{p,q}$  is a convex function penalising abrupt shape changes in  $S$  between neighbouring columns  $p$  and  $q$ . The training shapes are aligned in polar coordinates and the radial differences between neighbouring columns are computed at each column (equivalent to first order derivative). The radial differences between neighbouring columns,  $p$  and  $q$ , are generalised using mean  $m_{p,q}$  and standard deviation  $\sigma_{p,q}$ . These statistics are then used in determining maximum and minimum distances when connecting neighbouring columns in graph construction, i.e.  $\bar{\Delta}_{p,q} = m_{p,q} + c \cdot \sigma_{p,q}$ ,  $\underline{\Delta}_{p,q} = m_{p,q} - c \cdot \sigma_{p,q}$ , and  $c$  is a real constant. However, these inter-column arcs alone will impose hard constraint on shape regularisation. Hence, additional inter-column arcs are necessary in order to allow smooth transition between columns, that is intermediate values  $h$  in the range of  $\bar{\Delta}_{p,q}$  and  $\underline{\Delta}_{p,q}$  are used to construct inter-column arcs. The direction of these arcs is based on the first order derivative of the function  $f_{p,q}(h)$ . For each value of  $h$ , if  $f'_{p,q}(h) \geq 0$  an arc from  $V(x,y)$  to  $V(x+1, y-h)$  is established and if the  $f'_{p,q}(h) \leq 0$  the arc is connected from  $V(x+1, y)$  to  $V(x, y+h)$ . The weight for these arcs is assigned as the second derivative of the function  $f_{p,q}$ . Here, we employed a quadratic function,  $f_{p,q} = 3(x - m_{p,q})^2$ .

## 2.3 Feature Extraction

The media layer is usually thin and generally dark in intensity, and the adventitia layer tends to be brighter. However, acoustic shadow, calcification, and other interfering image features are common. Hence, the feature extraction is concerned with enhancing the difference between media and adventitia and suppressing undesirable features.

*First order derivative of Gaussian* – This set of filters is designed to highlight the intensity difference between media and adventitia. Four different orientations are used.

*Band-pass log-Gabor* – Log Gabor is used as a band-pass filter in three scales to enhance the border and to reduce speckles and other image artefacts. To minimize possible overlap with the derivate of Gaussian filter in extracting edge features, this process is carried out in coarser scales. Hence, these features highlight dominant edges.

*Local phase symmetry feature* – Symmetry feature [6] is exist in the frequency components at either the minimum or maximum symmetric points in their cycles, obtained by convolving even  $e_m(x,y)$  and odd  $o_m(x,y)$  symmetric Log Gabor filter to remove DC component and preserve phase in localised frequency. In [7] employs spatio-temporal technique to enhance edge and bar-like features and suppress speckles in ultrasound images.

Feature symmetry favours bar-like image patterns, which is useful in extracting the thin media layer. We modify the feature symmetry equation in [6] to focus only on the dark polarity (minimum intensity) symmetry:

$$FS(x,y) = \sum_m \frac{[|-e_m(x,y)| - |o_m(x,y)|] - T_m}{A_m(x,y) + \epsilon} \quad (2)$$

where  $m$  denotes filter orientation,  $\epsilon$  is a small constant,  $T_m$  is an orientation-dependent noise threshold,  $A_m(x,y) = \sqrt{e_m^2(x,y) + o_m^2(x,y)}$  and  $[\cdot]$  denotes zeroing negative values.

## 2.4 Cost function

The cost function indicates the likelihood of each node in the graph belongs to the minimum cost path that represents the desired interface. For segmenting the media-adventitia border, all the three types of features described in Sect. 2.3 are used. It takes the following form:

Table 1: Quantitative comparison. AD: area difference in percentage; AMD: absolute mean difference in pixel compared to ground-truth.

	No Shape Prior		Shape Prior	
	AD	AMD	AD	AMD
Mean	8.96	16.32	<b>4.91</b>	<b>6.89</b>
Std.	5.79	12.82	1.94	2.57
Min	3.26	4.33	2.35	3.56
Max	20.25	46.88	9.57	11.97

$$C(x, y) = C_d(x, y) + \alpha_1 C_G(x, y) + \alpha_2 (1 - FS(x, y)) \quad (3)$$

where  $C_d$  denotes the term for derivative of Gaussian features,  $C_G$  is for log-Gabor, and  $\alpha_1$  and  $\alpha_2$  are constants. The derivatives of Gaussian responses from different orientations are summed together to form  $C_d$ .  $C_G$  can be obtained by cascading the filtering responses across scales. However, more weight can be assigned to coarser scale features so that it presence the connectivity of media-adventitia border at the existence of acoustic shadow, e.g.  $C_G = G^{(3)} + G^{(4)} + 1.5G^{(5)}$  as used here and  $G^{(i)}$  denotes  $i$ th scale. Feature symmetry  $FS$  is useful in enhancing the thin layer of media. It is normalized beforehand, and since the middle of the layer has larger values  $1-FS$  is used in the cost function so that the interface between media and adventitia is highlighted. Note that each of the term in the cost function is normalized.

## 2.5 Compute the optimal interface

Each graph node is weighted by a value represents its rank to be selected in the minimum closed set graph, whose upper envelope corresponds to the optimal interface. The weight assignment is carried out according to  $w(x, y) = C(x, y) - C(x, y - 1)$  where  $w$  is the weight for each node in the directed graph, which serves as the base for dividing the nodes into non-negative and negative sets. The  $s-t$  cut method [1] can then be used to find the minimum closed set. The source  $s$  is connected to each negative node and every non-negative node is connected to the sink  $t$ , both through a directed arc that carries the absolute value of the cost node itself. The optimal media-adventitia interface corresponds to the upper envelope of the minimum closed set graph.

The segmented media-adventitia may still contain local oscillations. Smoothing can be applied to eliminate such oscillations. Here, RBF interpolation using thin plate base function is used to effectively obtain the final interface. Note, due to the images have been transformed into polar coordinates, the RBF processing only needs to be carried out in 1D.

## 3 Experimental Results

The proposed method is evaluated on a set of 40 IVUS images from 4 pullbacks acquired by a 40 MHz transducer Boston scientific ultrasound machine, where 20 images are used in the training set and the rest for testing. These images contain various forms of soft and fibrous plaque, and calcification. The training shapes are pre-aligned when transforming from Cartesian coordinates to polar coordinates. Due to the graph construction is defined according to the learned information and remained fixed during the segmentation, we limit the work on single template. Manual segmentation was carried out on all the images to establish a "ground-truth". The proposed method is compared with segmentation using the same graph construction but without incorporating the shape prior. Fig. 1 shows typical performance for both methods. Table 1 provides a quantitative comparison for media-adventitia border segmentation. The advantage of using prior is evidently clear. A qualitative comparison between manual labelling of the media-adventitia border and the proposed method is

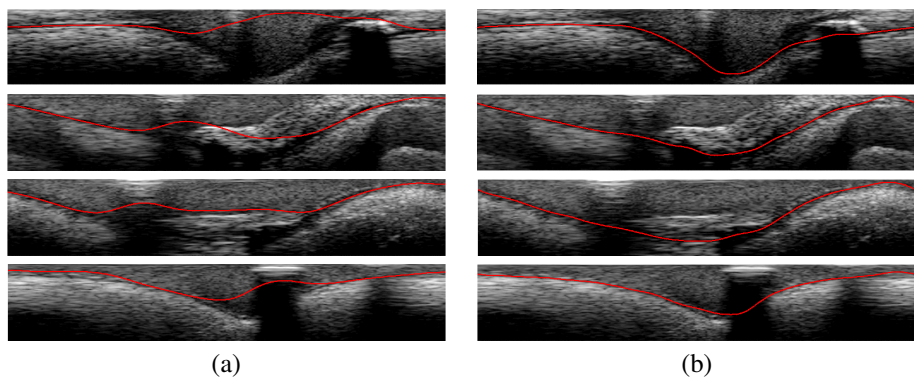


Figure 1: Media-adventitia border segmentation (a) without shape prior; (b) with shape prior.

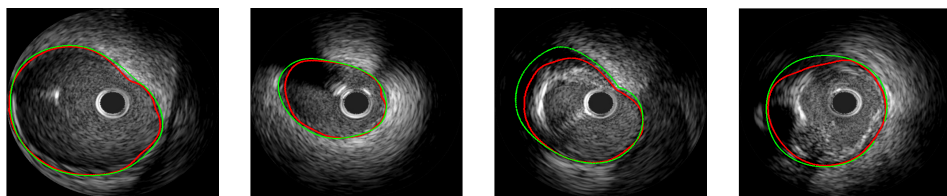


Figure 2: Comparison between ground-truth (green) and the proposed method (red).

shown in Fig. 2. Overall, the proposed method achieved promising results without any user initialisation and the use of shape prior provides better accuracy and consistency.

## 4 Conclusion

We presented an automatic media-adventitia segmentation method, whose geometric constrain is derived from the training set and integrated in the graph construction. Shape prior information helps to overcome the difficulties in finding the location of the border when there is calcification or guide wire shadowing. Qualitative and quantitative comparison showed superior performance of using shape prior and demonstrated a promising approach to IVUS image segmentation.

## References

- [1] Y. Boykov and V. Kolmogorov. An experimental comparison of min-cut/max- flow algorithms for energy minimization in vision. *IEEE T-PAMI*, 26(9):1124–1137, 2004.
- [2] Gozde Unal et al. Shape-driven segmentation of the arterial wall in intravascular ultrasound images. *IEEE Tran. Info. Tech. Biomed.*, 12(3):335–347, 2008.
- [3] K. Li et al. Optimal surface segmentation in volumetric images—a graph-theoretic approach. *IEEE T-PAMI*, 28(1):119–134, 2006.
- [4] Q. Song et al. Simultaneous searching of globally optimal interacting surfaces with shape priors. In *Proc. CVPR*, 2010.
- [5] Daniel Freedman and Tao Zhang. Interactive graph cut based segmentation with shape priors. In *Proc. CVPR*, pages 755–762, 2005.
- [6] Peter Kovesi. Symmetry and asymmetry from local phase. In *Proc. Tenth Australian Joint Conference on Artificial Intelligence*, 1997.
- [7] M. Mulet-Parada and J. Noble. 2D +T acoustic boundary detection in echocardiography. *Medical Image Analysis*, 4(1):21–30, 2000.